Ion irradiation damage in Er-doped silica probed by the Er^{3+} luminescence lifetime at 1.535 μm

A. Polman
FOM-Institute for Atomic and Molecular Physics, Kruislaan 407, 1098 SJ Amsterdam, The Netherlands, and AT&T Bell Laboratories, 600 Mountain Avenue, Murray Hill, New Jersey 07974

J. M. Poate
AT&T Bell Laboratories, 600 Mountain Avenue, Murray Hill, New Jersey 07974

(Received 24 August 1992; accepted for publication 19 October 1992)

The effect of MeV ion irradiation damage on the luminescence lifetime of erbium-doped silica glass films has been studied. The 10-μm-thick films were first implanted with 3.5 MeV Er at a fluence of 5×10^{15} cm^{-2}. When optically pumped at 488 nm, the films show a clear photoluminescence spectrum centered around 1.535 μm, corresponding to the $^4I_{13/2}\rightarrow{}^4I_{15/2}$ transition of $Er^{3+}(4f^{11})$, with a luminescence lifetime of 5.5 ms. After thermal annealing at 900 °C, the lifetime increases to 14.1 ms. Radiation damage was then introduced in the annealed films using 1 MeV He, 3.5 MeV C, 5.5 MeV Si, or 8.5 MeV Ge ions. The lifetime is decreased by irradiation with fluences as low as 10^{11} ions/cm^2 and continues to decrease with fluence until saturation occurs above $\approx10^{14}$ ions/cm^2. The saturation lifetime is ion-mass dependent and ranges from 6.6 to 8.5 ms. The lifetime changes are explained in terms of nonradiative energy transfer processes caused by irradiation-induced defects in the silica. A model for lifetime changes as a function of ion fluence is derived, assuming an inverse relation between the nonradiative lifetime and the defect density. Fits to the data show that the defect generation rate is a sublinear function of the ion fluence. The ion damage effects are governed by the electronic component of the energy loss along the ion trajectories.

I. INTRODUCTION

An understanding of the effects of ionizing radiation on silica glass is important in several technological fields. SiO_2 dielectric layers are routinely used in the fabrication of microelectronic devices, and their threshold voltage and leakage behavior can be influenced by irradiation. Silica-based containers are used in nuclear waste container technology because of the known mechanical resistance of these glasses to irradiation.[1] Furthermore, silica-based optical fibers are the standard in telecommunication technology, and radiation defects can give rise to significant transmission losses in the fibers.[2–4]

In this article the effect of MeV ion irradiation damage on the optical properties of Er-doped silica films is studied. Erbium-doped silica glass has recently attracted attention because of its use in optical fiber amplifiers.[5,6] Erbium, when incorporated as a trivalent ion, shows an optical transition at 1.5 μm, coinciding with the wavelength for minimum loss of standard optical telecommunications silica fiber. We have recently shown[7–9] that planar silica films can also be doped with Er, using MeV ion implantation. Such films have the potential to be used for the fabrication of a planar optical amplifier, which can then be integrated with passive devices on the same substrate.[10] After proper annealing treatment, Er-implanted silica films show sharply peaked photoluminescence spectra centered around 1.5 μm with relatively long luminescence lifetimes on the order of 10 ms. As will be shown in this work, the Er luminescence lifetime is a very sensitive measure of the defect structure in silica after ion irradiation.

Radiation damage in silica glass caused by electrons, neutrons, x rays, γ rays, ultraviolet (UV) radiation, and keV-MeV ions has been studied since the early 1950's. The measurements include[11] optical absorption and electron spin resonance spectroscopic data that determine the nature and structure of point defects and network distortions in silica,[2,12–15] as well as studies of refractive index changes[16,17] and macroscopic deformation upon irradiation.[18,19] A variety of radiation-induced defects in SiO_2 have now been characterized, such as for instance E' and B_2 oxygen vacancy centers, peroxy radicals, and nonbridging oxygen-hole centers.

In the present work, changes in the optical properties of the rare-earth dopant are used to study the evolution of radiation damage in silica, introduced by MeV He, C, Si, or Ge ions. By using a wide range of ion masses, the radiation damage behavior is correlated to electronic and nuclear stopping processes. Structural changes affecting the lifetime are observed at an extremely low irradiation fluence ($\approx10^{11}$ ions/cm^2) and eventually saturate at a higher fluence ($>10^{14}$ ions/cm^2). The role of defects on radiative and nonradiative luminescence decay processes is discussed, and a model is derived that relates the lifetime changes to the damage evolution during irradiation.

II. EXPERIMENT

Amorphous SiO_2 films, 10 μm thick, were grown on Si(100) substrates by thermal oxidation in a high-pressure steam ambient.[20] Subsequently, 3.5 MeV Er ions were implanted at room temperature to a total fluence of 5×10^{15} Er ions/cm^2. The Er concentration profile as a function of depth was measured with Rutherford backscattering spec-

 0021-8979/93/041669-06$06.00 © 1993 American Institute of Physics

Downloaded 15 Sep 2003 to 131.215.237.184. Redistribution subject to AIP license or copyright, see http://ojps.aip.org/japo/japcr.jsp

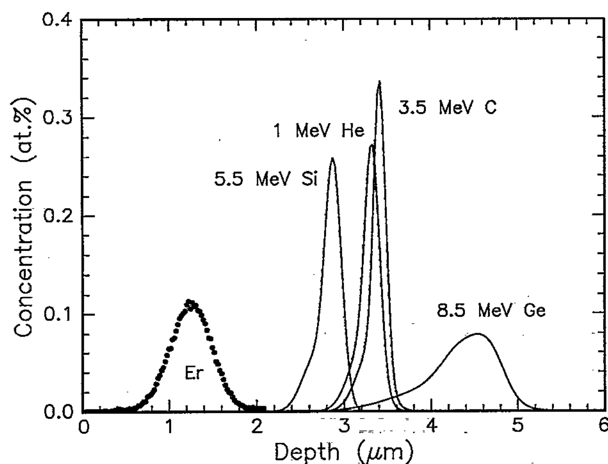

FIG. 1. Er concentration as a function of depth as measured by Rutherford backscattering spectrometry for a silica film implanted with 3.5 MeV Er ions/cm^2 at a fluence of 5.0×10^{15} ions/cm^2. Also shown are TRIM89 calculations of the ion ranges for the He, C, Si, and Ge irradiations used in this study (for a fluence of 5.0×10^{15} ions/cm^2).

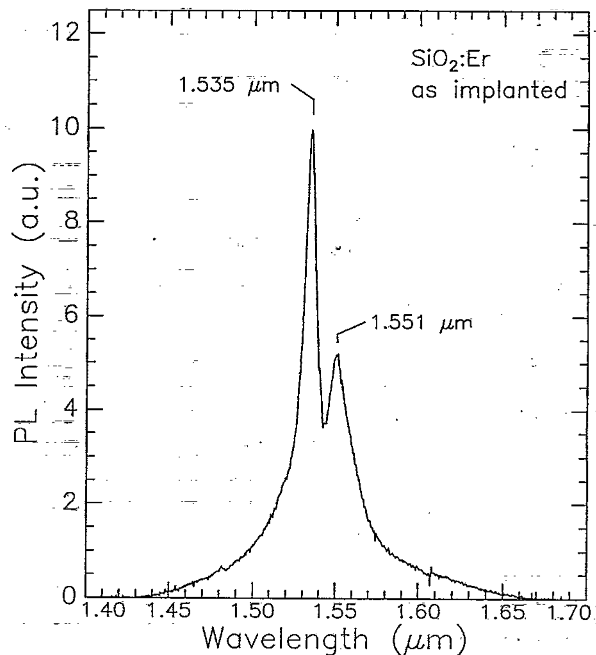

FIG. 2. Room-temperature photoluminescence spectrum for an Er-implanted (5.0×10^{15} ions/cm^2, 3.5 MeV) silica film (λ_{pump}=488 nm, spectral resolution 10 Å).

trometry (RBS) and is shown in Fig. 1. It is approximately Gaussian, centered at a depth of 1.25 μm, with a full width at half-maximum of 0.56 μm. The peak Er concentration was 0.11 at. %. After implantation, samples were annealed in vacuum for 1 h at 900 °C. This did not result in any measurable change in the Er profile. Radiation damage was introduced after annealing, using 1 MeV He, 3.5 MeV C, 5.5 MeV Si, or 8.5 MeV Ge ions from a 5SDH-4 National Electrostatics Corporation tandem accelerator. The implantation profiles for these ions have been calculated using Monte Carlo simulations (TRIM89)[21] and the results are indicated in Fig. 1. As can be seen, the ion ranges are 3.3, 3.4, 2.9, and 4.5 μm, respectively, and there is no overlap between the Er profile and the implanted He, C, Si, or Ge profiles. TRIM simulations also show that for these high-energy irradiations, the nuclear and electronic stopping profiles as a function of depth (not shown) are relatively constant in the Er-doped region.

Samples were analyzed with photoluminescence (PL) spectroscopy using the 488 nm line of an Ar^+ laser as a pump source. This line is absorbed near the $^4F_{7/2}$ manifold of Er^{3+}. The luminescence was detected using a 0.75 m SPEX monochromator and a liquid-nitrogen-cooled Ge detector, the total system resolution being 10 Å. The 150 mW pump signal was mechanically chopped at 10 Hz and the signal was collected using a lock-in amplifier. Luminescence decay measurements were performed at a wavelength of 1.535 μm using a 1.5 W, 2.0 ms pump pulse with a 800 μs fall time, also obtained using mechanical chopping. Decay curves were averaged and recorded using a digital storage oscilloscope. Decay measurements were also performed as a function of temperature in the range 78–298 K using a liquid-nitrogen cooled cryostat.

III. RESULTS

Figure 2 shows a PL spectrum of the silica film after Er implantation. The spectrum shows luminescence around 1.54 μm, characteristic of transitions between the first excited manifold $^4I_{13/2}$ and the $^4I_{15/2}$ ground manifold of Er^{3+} ($4f^{11}$) (Ref. 22). The spectrum is relatively sharp because the $4f$ orbitals of Er^{3+} are effectively shielded from the host by the outerlying closed $5s^2$ and $5p^6$ shells. The spectral width and double peak structure are due to Stark splitting and additional homogeneous and inhomogeneous broadening. The PL spectrum for the sample after annealing at 900 °C was essentially the same, except for the integrated PL intensity which was 3–4 times higher for the annealed sample. This will be discussed later.

Figure 3 shows luminescence decay measurements of the as-implanted and the annealed sample, both measured at 1.535 μm. As can be seen, a single exponential decay is observed in both cases, with $1/e$ decay times of 5.5 and 14.1 ms for the as-implanted and annealed samples, respectively. We have previously studied the annealing characteristics of these Er-implanted films in detail,[7] and found that changes in lifetime occur in a temperature window in which implantation-induced point defects (e.g., E' and B_2 centers) are known to anneal out. Therefore, we believe that the luminescence lifetime is related to the structure and density of the Er implantation-induced defects.

After having produced Er-doped silica films in the high-lifetime state by annealing out the defects, defects were reintroduced in a controlled manner using irradiation with He, C, Si, or Ge ions with fluences varying over seven orders of magnitude (10^{10}–10^{17} ions/cm^2). Figure 4 shows the luminescence lifetimes measured after C, Si, or Ge irradiation as a function of ion fluence. During 5.5 MeV Si irradiation, the lifetime remains unaltered at 14.1 ms up to

Downloaded 15 Sep 2003 to 131.215.237.184. Redistribution subject to AIP license or copyright, see http://ojps.aip.org/japo/japcr.jsp

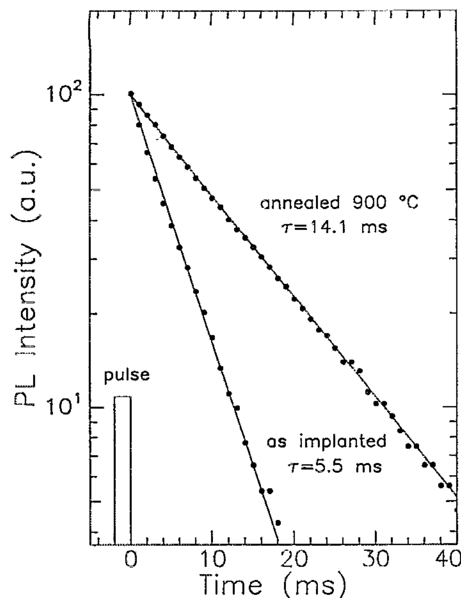

FIG. 3. Luminescence decay measured at $\lambda = 1.535$ μm of as-implanted and annealed (900 °C, 1 h) SiO_2:Er films. The timing of the excitation pulse ($\lambda = 488$ nm) is indicated schematically.

fluences of 10^{10} ions/cm^2. At higher fluences, the lifetime decreases and eventually saturates at 7.4 ms after irradiation with more than 10^{14} Si ions/cm^2. Similar behavior is seen for C and Ge implants. However, the lifetime at saturation and the fluence required for saturation are different for each ion. There are two important features: (1) The damage rate for light ions is smaller than for heavier ions, and (2) the lifetime at saturation decreases with increasing ion mass. The lifetime of the unannealed Er-implanted sample (5.5 ms indicated by a dashed line in Fig. 4) also fits in with this sequence. The lifetime of samples irradiated with 1 MeV He ions at fluences of 10^{16} and 10^{17} cm^{-2} was also measured. A saturation value of 8.5 ± 1 ms was found for both fluences. This value is also indicated in Fig. 4. In addition, low-temperature measurements of the lifetime were performed on samples that were as-implanted, annealed and reirradiated (3×10^{15} Si/cm^2). In all samples, the lifetime increased by around 1.5 ms on cooling from 300 to 78 K. This will be discussed later.

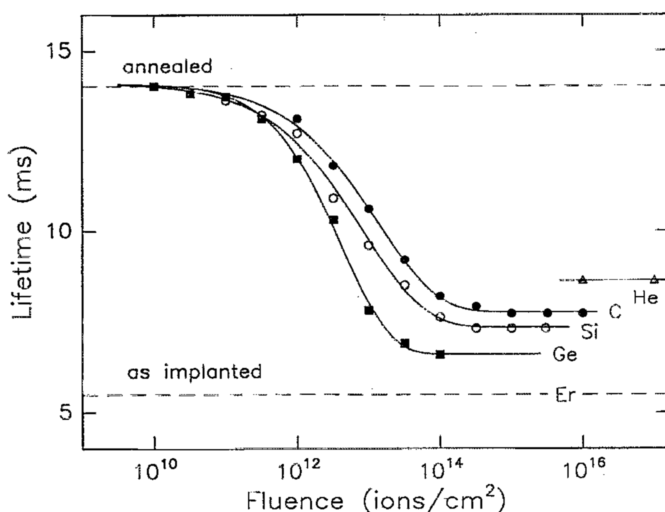

FIG. 4. (a) Luminescence decay times of annealed SiO_2:Er films after irradiation with 1 MeV He (triangles), 3.5 MeV C (closed circles), 5.5 MeV Si (open circles), or 8.5 MeV Ge (squares) ions, as a function of fluence. The lifetimes for as-implanted and annealed films are indicated by dashed lines. The drawn lines are calculated using Eq. (7).

IV. ANALYSIS

A. Radiative versus nonradiative lifetime

These data show that the luminescence lifetimes are sensitive probes of the defect structure of the irradiated samples. The intra-$4f$ transitions are forbidden from electric dipole radiation by the parity selection rule, but as a result of the mixing of other states into the $4f^{11}$ states, finite, but relatively long lifetimes are observed. The typical radiative lifetime for the $^4I_{13/2} \rightarrow {}^4I_{15/2}$ transition of Er^{3+} in silica-based glasses is in the order of 10–15 ms.[6] However, the measured lifetime may be lower as a result of fast nonradiative processes that quench the luminescence. For instance, phonon-assisted decay can reduce the lifetime. This decay has a distinct temperature dependence that depends on the number and energy of phonons necessary for the $^4I_{13/2} \rightarrow {}^4I_{15/2}$ transition. As the lifetime does not show a strong temperature dependence, it is concluded that these phonon-assisted processes do not play an important role in the Er-implanted silica films. Measurements on other Er-doped materials have shown a similar result.[6,23] Also, the lifetime can be reduced by concentration quenching effects that include energy transfer between Er ions and cooperative upconversion at high Er concentration and pump power.[6] These processes can be neglected at the low Er concentrations and pump powers used in the present experiments.

Furthermore, a nonradiative decay, reducing the measured lifetime, can occur if energy is transferred from excited Er^{3+} ions to acceptor states in the host[24] such as defects introduced by the ion beam. The nonradiative interaction term can take various functional forms depending on the interaction mechanism and in general, if the interaction depends on the distance between donor and acceptor, will lead to a nonexponential decay of the PL intensity $I(t)$ after pulsed excitation. As can be seen in Fig. 3, the decays in our experiments are purely exponential. This corresponds to a special case, in which the interaction has no radial dependence, described by the Stern–Volmer model.[24] In this case $I(t)$ takes the simple form

$$I(t) = I(t=0)e^{-t/\tau} \tag{1}$$

with

$$\frac{1}{\tau} = \frac{1}{\tau_r} + \frac{1}{\tau_{nr}}, \tag{2}$$

in which τ, τ_r, and τ_{nr} are the measured, the radiative, and the nonradiative lifetimes, respectively.

Downloaded 15 Sep 2003 to 131.215.237.184. Redistribution subject to AIP license or copyright, see http://ojps.aip.org/japo/japcr.jsp

TABLE I. Threshold fluences (ϕ_t, defined in Sec. IV B) determined from the curves in Fig. 4, together with calculated average nuclear (γ_n) and electronic (γ_e) energy deposition rates. The fit results for τ_{sat}, n, and c in Eq. (7) are also indicated.

Ion	ϕ_t (10^{12} cm^{-2})	γ_n (eV/ion Å)	γ_e (eV/ion Å)	τ_{sat} (ms)	n	c (cm^2)^n
3.5 MeV C	7.8	0.16	133	7.7	0.63	2.1×10^{-9}
5.5 MeV Si	4.5	1.2	214	7.3	0.62	3.5×10^{-9}
8.5 MeV Ge	3.0	4.5	210	6.6	0.83	1.6×10^{-11}

From rate equation arguments,[24] it follows that the PL intensity is proportional to τ/τ_r. Our previous annealing studies of the present implanted films have shown that an increase in the measured lifetime τ is always accompanied by a similar increase in PL intensity.[7] This then indicates that τ_r does not change upon annealing. Hence, from Eq. (2) it follows that changes in lifetime are mainly due to changes in the nonradiative lifetime τ_{nr}. In further support of this argument is the observation that the shape of the PL spectrum does not change upon annealing.

B. Electronic versus nuclear stopping

From the C, Si, and Ge data in Fig. 4, the threshold fluences ϕ_t have been estimated, defined as the fluence necessary to reduce the lifetime to a value halfway between the initial and final values. The fluence ϕ_t is listed in Table I for the three irradiation conditions and ranges from 3.0×10^{12} to 7.8×10^{12} ions/cm^2. To quantify these numbers, the energy loss profiles for C, Si, and Ge in SiO_2 were calculated using TRIM89 and convoluted with the Er concentration profile as measured with RBS (Fig. 1). In this way, the average lattice vacancy formation rate due to nuclear displacements (γ_n) and the average ionization rate due to electronic energy loss (γ_e) around the Er ions were calculated. The results are listed in Table I. For a given implantation fluence, γ_n varies by a factor 28 for the three different ions while γ_e varies by only a factor 1.6. Given the fact that ϕ_t varies only by a factor ≈2.6, it is concluded that the electronic interactions play a dominant role in determining the lifetime changes after ion irradiation. For each ion (C, Si, or Ge), the electronic energy deposition density can be estimated at which the threshold fluence is reached, i.e., $\gamma_e\phi_t$. Using the parameters in Table I, values in the range $(0.6\text{–}1.0)\times10^{23}$ eV/cm^3, i.e., ≈0.9–1.5 eV/atom are found.

C. Damage model

In order to quantitatively analyze the irradiation-induced lifetime changes as a function of fluence, assumptions need to be made about the relation between the lifetime and the defect concentration, and on the defect concentration as a function of ion fluence. In the Stern–Volmer model, the nonradiative lifetime is inversely proportional to the defect concentration d:

$$\tau_{nr}=\frac{a}{d}, \qquad (3)$$

with a a proportionality constant. There are several models for the dependence of d on the ion fluence ϕ. In the most simple model, each ion damages a certain volume of the material to its maximum damage level. In the low-fluence approximation, the volume fraction of material damaged to saturation is then $f=b\phi$, with b a proportionality constant. A more complicated model takes into account damage annihilation by interaction between damaged regions. This interaction causes the damage produced per ion to decrease as the material becomes more damaged leading to a sublinear increase of $f(\phi)$, which is often modeled by a power dependence $f=b\phi^n$, with $0<n<1$. Furthermore, in the limit of high-fluence irradiation, as saturation is approached,[25] the damage increase with fluence must be corrected for the fraction of material that has already been damaged to saturation: $(1-f)$. In a general formulation, the damage rate can then be described by

$$\frac{df}{d\phi}=c\phi^{n-1}(1-f), \quad 0<n\leqslant1, \qquad (4)$$

with f the damaged fraction, c a proportionality constant, and n determining the degree of nonlinearity ($n=1$ corresponds to a constant damage rate as a function of dose). This leads to

$$f=1-\exp\left(-\frac{c}{n}\phi^n\right). \qquad (5)$$

Note that the exponential term, known as a stretched exponential, is often used in amorphous materials to describe property changes and interactions governed by a spectrum of activation energies or relaxation times. From Eq. (5) it follows that the defect concentration is given by

$$d(\phi)=d_{sat}\left[1-\exp\left(-\frac{c}{n}\phi^n\right)\right], \qquad (6)$$

with d_{sat} the saturation defect density. By substituting Eq. (6) in Eq. (3), and Eq. (3) in Eq. (2), it follows that

$$\tau(\phi)=\tau_{sat}\Big/1+\left(\frac{\tau_{sat}}{\tau_0}-1\right)\exp\left(-\frac{c}{n}\phi^n\right). \qquad (7)$$

This equation has three free parameters: τ_{sat}, the saturation lifetime for high-fluence irradiation, n, and c. In the present experiments, the initial lifetime $\tau_0=14.1$ ms. The best fits of this equation to the curves in Fig. 4 are shown as drawn lines in the figure. The fit parameters are listed in Table I.

As can be seen, the model in Eq. (7) describes the data quite well. The relatively slow decrease of the lifetime over

Downloaded 15 Sep 2003 to 131.215.237.184. Redistribution subject to AIP license or copyright, see http://ojps.aip.org/japo/japcr.jsp

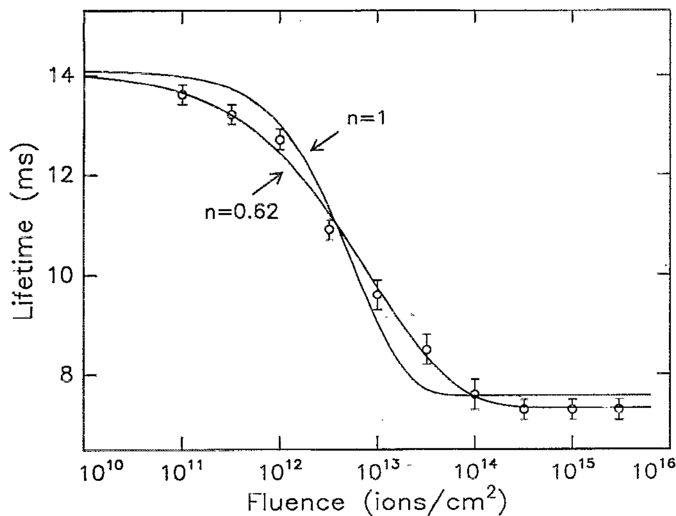

FIG. 5. Same data for Si irradiation as in Fig. 4, with fits according to Eq. (7) for $n=0.62$ and $n=1$.

a dose range of three orders of magnitude results in n values smaller than 1, i.e., the damage increases sublinearly with ion fluence. To illustrate the sensitivity of the fit results, Fig. 5 shows the data for Si again, with fits using $n=0.6$ (best-fit value) and $n=1$. It is clear that the latter curve does not describe the data well. As can be seen from Table I, the deviation from linearity is larger for the lighter ions ($n\approx0.6$ for C and Si) than for the heavier ion ($n=0.8$ for Ge).

V. DISCUSSION AND COMPARISON WITH OTHER EXPERIMENTS

The nonlinear increase of damage with ion fluence is in agreement with earlier work by EerNisse *et al.*[19] who have found a sublinear ($n\approx0.9$) compaction in silica caused by electron irradiation. Indeed, in the present experiments, electronic excitation is the main energy loss factor (see Table I) and in fact the largest sublinearity (lowest n) is found for irradiation conditions where electronic energy loss is most dominant. Similar sublinear behavior is also observed for electrons and x rays[26] as well as for γ irradiation[2,12] of silica.

As discussed in Sec. IV B, the electronic energy deposition density at which the irradiation-induced effects start to saturate is in the order of 10^{23} eV/cm^3. This number is in very good in agreement with the energy density at which radiation-induced compaction,[18] as well as the density of E' centers,[13] saturate after irradiation.

Figure 4 clearly shows the differences in saturation damage for the four different irradiation conditions as reflected in the saturation lifetime τ_{sat}. The fact that the high-energy heavy ions create heavier damage than the lower-energy lighter ions may be explained by differences in the collision cascade density, differences in damage interaction with precursor damage in the silica,[12,14] or differences in interaction of damage produced by electronic and nuclear stopping.[18,26] These results are corroborated by work by Chengru *et al.*,[13] who have shown that the maximum E' density increases with increasing ion mass and energy. It is important to realize that the irradiation fluence for 1 MeV He, which causes a significant decrease in the lifetime, is a typical fluence required for taking an RBS spectrum using a 1 MeV He beam. This implies that the optical properties of these Er-doped materials are severely affected by RBS analysis. The observation that the luminescence lifetime can be "tuned" to the desired value using ion irradiation may be of use if electroluminescence devices based on Er-doped silica would be fabricated.

Finally, it is interesting to compare these results with those on radiation damage in amorphous Si (a-Si), which is also covalently bound, but semiconducting rather than insulating. Roorda *et al.*[27] have studied the derelaxation of a-Si as a function of ion fluence and mass using Raman spectroscopy. This derelaxation of the a-Si network results from the introduction of defects and scales with the nuclear stopping power. The changes in defect structure were observed at 10–400 times higher ion fluence for the same irradiation conditions as described in the present article. Stolk *et al.*[28] have studied this phenomenon in further detail by measuring the carrier lifetime in ion-damaged a-Si and found that changes in lifetime were quite well described by a model as in Eq. (7) with $n=1$. Comparing with these data it is concluded that the response of the SiO_2 network to ion damage is quite different than that of a-Si.

VI. CONCLUSIONS

Ion irradiation damage by MeV He, C, Si, and Ge ions in Er-doped silica glass has been studied using measurements of the luminescence lifetime of the intra-4f transition of Er^{3+} at 1.535 μm. The annealed, undefected material shows a lifetime of 14.1 ms. The lifetime is decreased by irradiation with fluences as low as 10^{11} ions/cm^2 and continues to decrease with fluence until saturation occurs above $\approx10^{14}$ ions/cm^2. The saturation lifetime is ion-mass dependent and ranges from 6.6 to 8.5 ms. The defect generation rate is a sublinear function of the ion fluence and described by a stretched exponential with n in the range 0.6–0.8 and the ion damage effects are governed by the electronic component of the energy loss along the ion trajectories.

ACKNOWLEDGMENTS

Work at the FOM-Institute is part of the research program of the Foundation for Fundamental Research on Matter (FOM) and was supported by the Netherlands Technology Foundation (STW) and the IOP Electro-Optics Programme of the Ministry of Economic Affairs. C. A. Volkert is acknowledged for stimulating discussions.

[1] H. Matzke, in *Ion Beam Modification of Insulators*, edited by P. Mazzoldi and G. W. Arnold (Elsevier, Amsterdam, 1987), p. 501.
[2] D. L. Griscom and E. J. Friebele, Radiat. Eff. **65**, 63 (1982).
[3] S. Karasawa, N. Horiuchi, and T. Takada, Nucl. Instrum. Methods B **47**, 404 (1990).
[4] H. Böck, J. Siehs, and N. Vana, Radiat. Eff. **65**, 75 (1982).
[5] P. Urquhart, IEE Proc. **135**, 385 (1988).
[6] W. J. Miniscalco, J. Lightwave Technol. **9**, 234 (1991).

Downloaded 15 Sep 2003 to 131.215.237.184. Redistribution subject to AIP license or copyright, see http://ojps.aip.org/japo/japcr.jsp

[7] A. Polman, D. C. Jacobson, D. J. Eaglesham, R. C. Kistler, and J. M. Poate, J. Appl. Phys. **70**, 3778 (1991).
[8] A. Polman, D. C. Jacobson, A. Lidgard, J. M. Poate, and G. W. Arnold, Nucl. Instrum. Methods B **59/60**, 1313 (1991).
[9] M. A. Marcus and A. Polman, J. Non-Cryst. Solids **136**, 260 (1991).
[10] C. H. Henry, G. E. Blonder, and R. F. Kazarinov, J. Lightwave Technol. **7**, 1530 (1989).
[11] For a review, see G. W. Arnold and P. Mazzoldi, in *Ion Beam Modification of Insulators*, edited by P. Mazzoldi and G. W. Arnold (Elsevier, Amsterdam, 1987), p. 195.
[12] R. A. B. Devine, Nucl. Instrum. Methods B **46**, 244 (1990).
[13] Shi Chengru, M. Tan, and T. A. Tombrello, J. Non-Cryst. Solids **104**, 85 (1988).
[14] M. Antonini, P. Camagni, P. N. Gibson, and A. Manara, Radiat. Eff. **65**, 41 (1982).
[15] J. P. Duraud, F. Jollet, Y. Langevin, and E. Dooryhee, Nucl. Instrum. Methods B **32**, 248 (1988).
[16] U. Katenkamp, H. Karge, and R. Prager, Radiat. Eff. **48**, 31 (1980).
[17] P. D. Townsend, Nucl. Instrum. Methods B **46**, 18 (1990).
[18] E. P. EerNisse and C. B. Norris, J. Appl. Phys. **45**, 5196 (1974).
[19] E. P. EerNisse, J. Appl. Phys. **45**, 167 (1974).
[20] H. J. Lee, C. H. Henry, K. J. Orlowsky, R. F. Kazarinov, and T. Y. Kometani, Appl. Opt. **27**, 4104 (1988).
[21] J. P. Biersack and L. J. Haggmark, Nucl. Instrum. Methods **174**, 257 (1980).
[22] S. Hüfner, *Optical Spectra of Transparent Rare-Earth Compounds* (Academic, New York, 1978).
[23] M. J. Weber, Phys. Rev. B **8**, 54 (1973).
[24] J. C. Wright, in *Radiationless Processes*, edited by F. K. Fong (Springer, Berlin, 1976).
[25] F. F. Morehead, Jr. and B. L. Crowder, Radiat. Eff. **6**, 27 (1970).
[26] W. Primak and R. Kampwirth, J. Appl. Phys. **39**, 5651 (1968).
[27] S. Roorda, J. M. Poate, D. C. Jacobson, B. S. Dennis, S. Dierker, and W. C. Sinke, Appl. Phys. Lett. **56**, 2097 (1990).
[28] P. A. Stolk, L. Calcagnile, S. Roorda, W. C. Sinke, A. J. M. Berntsen, and W. F. van der Weg, Appl. Phys. Lett. **60**, 1688 (1992).

Downloaded 15 Sep 2003 to 131.215.237.184. Redistribution subject to AIP license or copyright, see http://ojps.aip.org/japo/japcr.jsp